

Contents

| | |
|--|------------|
| 摘要..... | i |
| Abstract..... | iii |
| Acknowledgements..... | v |
| Contents..... | vi |
| List of Tables..... | ix |
| List of Figures | x |
| Symbolic Interpretation..... | xiv |
| | |
| Chapter 1 Introduction | 1 |
| 1.1 Motivation | 1 |
| 1.2 AFM Review | 2 |
| 1.3 The Role of the Contact Potential in Non-Contact AFM | 6 |
| 1.4 Literature Review | 8 |
| | |
| Chapter 2 Experimental Apparatus..... | 14 |
| 2.1 Vacuum System | 14 |
| 2.2 Scanning Tunneling Microscopy (STM)..... | 15 |
| 2.2.1 Introduction | 15 |
| 2.2.2 Feedback system..... | 15 |
| 2.2.3 Constant-current mode and constant-height mode | 17 |
| 2.2.4 Preparing STM tips..... | 19 |
| 2.3 Noncontact-Atomic Force Microscopy (NC-AFM) | 21 |
| 2.3.1 Introduction | 21 |
| 2.3.2 Feedback system..... | 23 |
| 2.3.3 Light beam adjustment | 24 |
| 2.3.4 The measurement of the spectroscopy | 26 |
| 2.3.5 Preparing AFM cantilevers..... | 29 |
| | |
| Chapter 3 Theories | 30 |
| 3.1 Principles of Electron Tunneling | 30 |
| 3.2 Principles of NC-AFM | 32 |
| 3.2.1 Introduction of FM-AFM | 32 |
| 3.2.2 Relation between frequency shift and forces..... | 33 |
| 3.3 Interaction Force between the Tip and the Sample..... | 36 |
| 3.4 Calculation of Interaction Force between Tip and Sample..... | 37 |
| 3.4.1 A tip-lever system..... | 38 |
| 3.4.2 $D(V_t)$ | 39 |

| | |
|--|-----------|
| Chapter 4 Apparent Topographic Height Variations as Measured by Atomic Force Microscopy over a Flat, Differentially Doped Silicon Surface | 41 |
| 4.1 Introduction | 41 |
| 4.2 Experiment | 44 |
| 4.2.1 Sample preparation | 44 |
| 4.3 Results and Discussion | 47 |
| 4.3.1 The relevant forces and force gradients..... | 47 |
| 4.3.2 Calculation of the tip-sample distance | 51 |
| 4.3.3 The origin of incorrect z -height measurement..... | 56 |
| 4.3.4 Experiment observation..... | 61 |
| 4.3.5 The tip-sample distance curves using conduction tips | 63 |
| 4.3.6 The apparent z -height deviation using conduction tips | 65 |
| 4.3.7 Using nonconductive tips | 65 |
| 4.4 Conclusion | 68 |
| Chapter 5 SiO₂/Si(111) Height Error by Atomic Force Microscopy | 69 |
| 5.1 Introduction | 69 |
| 5.2 Experiment | 70 |
| 5.3 Results and Discussion | 73 |
| 5.3.1 AFM images and line-profiles | 73 |
| 5.3.2 Tip Radius from $D(V_t)$ curve fitting | 82 |
| 5.3.3 The step height versus effective potential difference | 86 |
| 5.4 Conclusion | 89 |
| Chapter 6 Conclusion..... | 90 |
| 6.1 Apparent Topographic Height Variations as Measured by Atomic Force Microscopy over a Flat, Differentially Doped Silicon Surface | 90 |
| 6.2 SiO ₂ /Si(111) Height Error by Atomic Force Microscopy | 92 |
| Appendix A The Force Laws for Bodies of Different Geometries: the Hamaker Constant..... | 93 |
| Appendix B Constant Force Gradient..... | 97 |
| B.1 For Small Tip Oscillation Amplitude..... | 97 |
| B.2 Analytical Expressions for the Force and Force Gradient Using Different Models | 98 |
| Appendix C Do STM Mode Using Cantilever for Atomic Resolution | 99 |

| | |
|--|------------|
| Appendix D Additional Calculation..... | 100 |
| D.1 Apparent z -Height Deviation versus Tip Bias for Constant Force Gradient | 100 |
| D.2 Apparent z -Height Deviation versus Tip Bias for Non-Constant Force Gradient | 101 |
| D.3 Forces versus Tip-Sample Distance and Forces versus Degree..... | 102 |
| Bibliography. | 103 |
| Vita..... | 107 |



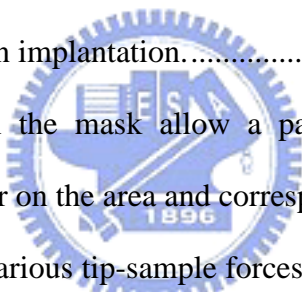
List of Tables

| | |
|--|----|
| Table I. Analytical expressions for the force and force gradient using different models for the tip shape. The formulas are valid for $D < R$ and zero contact potential. The right-hand column gives the variation in tip-sample separation with U for fixed force gradient. F : force, F' : force gradient, D : tip-to-sample separation, R : tip radius, q_{tip} : the tip open-cone angle, L : length of the tip, U : tip bias subtract contact potential, H : Hamaker constant, and ϵ_0 : vacuum permittivity..... | 98 |
|--|----|



List of Figures

| | |
|--|----|
| Fig. 1.1 Historical and present status for atomic force microscopy (AFM)..... | 4 |
| Fig. 1.2 Schematic models of (a) contact model AFM and (b) NC-AFM..... | 5 |
| Fig. 1.3 Definition and basic measurement setup of contact potential difference (CPD). | 7 |
| Fig. 1.4 The curve indicated by triangles show how the tip-to-sample separation D varies with sample voltages U at a constant force gradient of 0.06 N/m..... | 9 |
| Fig. 1.5 Least-squares fit of the vdW contribution, assuming $\Delta f_{vdW} \propto s^{-3/2}$ in the range 1-6nm..... | 10 |
| Fig. 1.6 Auxiliary sketches of (a) the lever-sample, (b) the cone-sample, and (c) the tip apex-sample system..... | 11 |
| Fig. 1.7 (a) SEM images corresponding to the symmetrical tip A used in the experiments. The images show a conical shape ended at a sphere of $R \sim 40$ nm. (b) Electrostatic normal force vs $1/D$ for different applied voltages..... | 12 |
| Fig. 1.8 Step heights as a function of V_{bias} measured by NC-AFM..... | 13 |
| Fig. 2.1 Two-dimensional diagram that illustrates the chamber consisting of loading chamber, preparative chamber, and observation chamber..... | 14 |
| Fig. 2.2 This is STM feedback system that acquires the tunneling current and control the z-piezo movement by $\Delta I-\Delta V$ transfer..... | 16 |
| Fig. 2.3 STM operation and schematic diagram..... | 18 |
| Fig. 2.4 The sketch of the etching procedure for the tungsten (W) tip..... | 20 |
| Fig. 2.5 (a) The effective distance for the different force. (b) Forces versus distance curve for different operation modes of AFM. Copied from internet..... | 22 |
| Fig. 2.6 AFM block diagram for getting the topography by the feedback system. | 23 |
| Fig. 2.7 Schematic diagram of the optical beam deflection. AFM deflection beam is adjusted | |

| | |
|--|----|
| on the position sensitive detector (PSD)..... | 25 |
| Fig. 2.8 Demonstration of the voltage dependence of the height displacement $Z(V_t)$ for two different materials on the surface..... | 26 |
| Fig. 2.9 Illustration of the voltage dependence of the frequency shift for two different materials on the surface..... | 27 |
| Fig. 2.10 $\Delta f(z)$ shows approaching trace of the frequency shift of the cantilever and $Q(z)$ | 28 |
| Fig. 2.11 OMICRON attaching device and positioning the cantilever chip..... | 29 |
| Fig. 3.1 Wavefunction for an election with kinetic energy $E=U/2$ penetrating a potential barrier U..... | 31 |
| Fig. 3.2 The Schematic view of an oscillating cantilever has definition of geometric terms...  | 35 |
| Fig. 3.3 The minimum tip-sample distance D calculated for various tip radii as indicated. | 40 |
| Fig. 4.1 The flow chart of Boron implantation..... | 45 |
| Fig. 4.2 (a) The windows on the mask allow a pattern for ion implantation. (b) SEM micrograph of the Si(100) wafer on the area and corresponding to (a)..... | 46 |
| Fig. 4.3 Log-log scale plot of various tip-sample forces for a spherical tip apex with radius (a) 5 (b) 20 (c) 100 nm..... | 49 |
| Fig. 4.4 Log-log scale plot of various tip-sample force gradients with tip radius R = (a) 5 (b) 20 (c) 100 nm..... | 50 |
| Fig 4.5 The minimum tip-sample distance D solved from (a) Eq. (4.3) and (b) Eq. (4.4) for f_0 $= 260$ kHz, $\Delta f = -30$ Hz, $k = 42$ N/m, and various tip radius R as indicated. | 53 |
| Fig. 4.6 Individual contribution to Δf from various component forces as indicated. | 55 |
| Fig. 4.7 (a) Schematic diagram showing a line profile when a tip scans over a flat conducting surface. (b) Tip-sample distances as a function of V_t on M_1 (cyan-long dash-line) and M_2 (pink-solid-line) and their differences (underneath green-line). | 58 |
| Fig. 4.8 The apparent topographic height deviation Δz as a function of V_t for various R | 59 |
| Fig. 4.9 The plateau height versus tip radius..... | 60 |

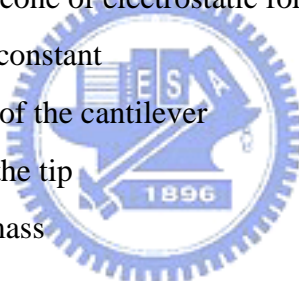
| | |
|--|----|
| Fig. 4.10 STM (labeled) and NC-AFM images for a diluted HF-etched Si(100) substrate with tip bias as indicated in volt | 62 |
| Fig. 4.11 Relative z -height (tip-sample distance D) versus tip bias measured on the n-type (z_n , cyan) and p-type (z_p , pink) domains | 64 |
| Fig. 4.12 Apparent z -height differences $\Delta z = z_n - z_p$ versus CPD | 67 |
| Fig. 5.1 (a). STM image for the Si(111)-(7×7) surface. (b) Zoom-in image from (a). (c) The line-profile between X-Y in (a). | 72 |
| Fig. 5.2 (a) The schematic showing a SiO_2 film was created by thermal oxidation. (b) Voids can be created by annealing ~800 °C for 5 ~ 10 mins..... | 72 |
| Fig 5.3 NC-AFM topography image ($250 \times 250 \text{ nm}^2$) of the SiO_2 films on the Si(111) surface using sharp Si tip. | 74 |
| Fig. 5.4 The relative step height is as function of tip bias for Si-tip. | 75 |
| Fig. 5.5 NC-AFM images ($250 \times 250 \text{ nm}^2$) were obtained by using sharp PtIr5 tip. | 77 |
| Fig 5.6 The relative step height is as function of tip bias for the sharp PtIr5-tip. | 78 |
| Fig 5.7 NC-AFM topography image ($300 \times 300 \text{ nm}^2$) of the SiO_2 films on the Si(111) surface using sharp PtIr5-tip. | 80 |
| Fig 5.8 The relative step height is as function of tip bias for blunt PtIr5-tip. For Blunt PtIr5-tip, there are different step heights were measured from the different tip bias. | 81 |
| Fig. 5.9 The CPD can be defined from the $D(V_t)$ for the PtIr5-tip. | 82 |
| Fig 5.10 (a) The sharp PtIr5-tip fitted with the calculation model of the weighted integral. The fitting radius is $R = 20 \text{ nm}$ for the sharp PtIr5-tip. (b) It is SEM picture for the sharp PtIr5-tip before scanning..... | 83 |
| Fig. 5.11 Tip sample distance as a function of the effective potential difference. | 85 |
| Fig. 5.12 The experimental data have good fitting with the calculation for $R = 20 \text{ nm}$ | 86 |
| Fig. 5.13 The relative step heights obtained from the AFM images between the SiO_2 and Si(111) regions..... | 88 |

| | |
|---|-----|
| Fig. A.1 (a) The model is Molecule near a wall. (b) The model is a spherical particle near a wall ($R >> D$) | 94 |
| Fig. C.1. The STM image is obtained by using AFM Si-cantilever. | 99 |
| Fig. D.1 The apparent topographic height deviation Δz is as a function of V_t with various R when the $F'_{ts} = (F_{s_sphere} + F_{vdW})' = const.$ | 100 |
| Fig. D.2 The apparent topographic height deviation Δz is as a function of V_t with various R when the $F'_{ts} = (F_{apex} + F_{tr_cone} + F_{vdW})' = nonconst.$ | 101 |
| Fig. D.3 (a) The force as a function of tip-sample distance (z) calculated for $R = 2.5$ nm, $U = 2.5$ V, $A = 16$ nm and $D = 1.718$ nm. (b) The force as a function of degree is transformed from (b) by $z = D + A + A \cos(\theta)$ | 102 |



Symbolic Interpretation

- A : cantilever oscillation amplitude
 A_{exc} : excitation amplitude
 D : minimum position between tip and sample
 E : an electron energy
 F : force
 F' : force gradient
 F_{chem} : chemical forces
 F_{cone} : cone of electrostatic force
 F_{vdw} : Van der Waals force
 F_{el} : long-ranged electrostatic force
 $F_{tr-cone}$: truncated-cone of electrostatic force
 H : Hamaker constant
 h : tip height of the cantilever
 l : length of the tip
 m : electron mass
 m^* : effective mass
 P_z : momentum in z direction
 Q : damping voltage
 R : radius of apex model
 R_s : radius of spherical model
 U : potential
 U : effective potential difference
 V_{cp} : contact potential
 V_{cpd} : contact potential difference
 V_{mcp} : mean contact potential
 V_{ts} : potential energy between tip and sample
 V_t : applied tip bias
 V_{sample} : applied sample bias
 x : x direction



y : y direction
 z : z direction
 Z : relative distance
 z : average tip-sample distance
 Δf : frequency shift
 Δz : apparent z-height differences
 $\Delta\Phi$: work function difference
 k : spring constant
 f_0 : cantilever free oscillation frequency
 e_0 : vacuum permittivity
 r : number of atoms per unit volume
 q_{tip} : cantilever full cone angle
 q_{lever} : angle of cantilever respect to sample surface
 Φ_{tip} : work function of the tip
 Φ_{sample} : work function of the sample

